Presented at the ISRM International Symposium 2006, November 8-10, Singapore

EXPERIMENTAL ASSESSMENT OF HEALING OF FRACTURES IN ROCK SALT

K. FUENKAJORN

Geomechanics Research Unit
Institute of Engineering, Suranaree University of Technology
111 University Avenue, Nakhon Ratchasima, Thailand30000
(kittitep@sut.ac.th)

The objective of this research is to assess experimentally the healing effectiveness of rock salt fractures as affected by the applied stresses, fracture characteristics, moisture contents and time. The effort involves (1) fracture pressurization tests under uniaxial and radial loading, (2) gas flow permeability tests to monitor the time-dependent behavior of the salt fractures, and (3) point loading and diameter loading tests to assess the mechanical performance of the fractures after healing. Tension-induced fractures and fractures formed by saw-cut surfaces and by polished surfaces have been prepared in salt specimens. Series of gas flow testing have been performed to monitor the changes of the fracture permeability under quasi-static loading ranging from 0.7 to 20 MPa for up to 120 hours. Healing tests under static loading have been carried out under both dry and saturated conditions. The results suggest that the primary factors governing the healing of salt fractures are the origin and purity of the fractures, and the magnitudes and duration of the fracture pressurization. Inclusions or impurity significantly reduce the healing effectiveness. The hydraulic conductivity of the fractures in pure salt can be permanently reduced by more than 4 orders of magnitude under the applied stress of 20 MPa for a relatively short period. For most cases the reduction of salt fracture permeability is due to the fracture closure which does not always lead to fracture healing. The closure involves visco-plastic deformation of the asperities on both sides of the salt fractures, while the healing is the covalent bonding between the two surfaces. Fracture roughness and moisture contents apparently have insignificant impact on the healing process.

Keywords: Healing; rock salt; fracture.

1. Introduction

Damage or fractures in rock salt formations can be healed under hydrostatic and non-hydrostatic compression. When cracks are closed, permeability can be reduced by several orders of magnitude. The healing capability of fractures is one of the advantages for rock salt to be used as a host rock for nuclear waste repository in the United States and Germany (Habib & Berest, 1993). The presence of damage in the form of micro-cracks in salt can alter the structural stability and permeability of salt, affecting the integrity of a repository (Chan *et al.*, 1998). The healing of rock salt fractures around the air or gas storage caverns also affects the designed storage capacity and the mechanical stability of the caverns (Katz & Lady, 1976). Miao *et al.* (1995) state that healing of rock salt is probably due to the visco-plastic deformation of grains, causing the closure of cracks and pore spaces. The size reduction of the micro-cracks can increase the salt stiffness and strength. The main driving force for fracture healing is a minimization of surface tension, and creation of contact areas and covalent bonds between the two surfaces of the fracture.

It is defined here that healing is the closure of fractures without any precipitation of materials inside. It is a chemical and physical process in which the material properties evolve with time or in which the defects (voids and cracks) decrease. The initiation, propagation and healing of fractures in salt mass around underground structures have long been recognized, most investigations however have been concentrated on their impact on the mechanical constitutive behavior of the rock (e.g., Allemandou & Dusseault, 1993; Munson *et al.*, 1999). Several experimental researches on the healing and consolidation of crushed salt have also been carried

out in an attempt at understanding the healing behavior between the salt particles and their impact on the bulk properties (e.g., Ouyang & Daemen, 1989; Miao *et al.*, 1995). A direct experimental assessment of the healing behavior of individual salt fractures remains rare.

The objective of this research is to assess experimentally the healing effectiveness of rock salt fractures as affected by the stress conditions, fracture types, and time. The effort involves healing tests under uniaxial and radial pressures, gas flow permeability tests to monitor the time-dependent behavior of the salt fractures, and point loading and diameter loading tests to assess the mechanical performance of the fractures after healing.

2. Salt Specimens

The salt specimens used here have been drilled from the Middle and Lower members of the Maha Sarakham Formation in the Sakhon Nakhon Basin, northeastern Thailand. Warren (1999) gives detailed descriptions of the salt and geology of the basin. The core specimens are from the depths ranging between 250 and 400 meters. The compressive and tensile strengths of the salt have been determined. These properties are needed for designing the healing test parameters. The nominal diameter of all specimens is 60 mm. The sample preparation and test procedures follow as much as practical the ASTM standard practices (i.e., ASTM D2938, D3967, D4543 and D5731). The uniaxial compressive strengths, Brazilian tensile strengths and point load strength index are determined as 30.3 MPa, 1.9 MPa and 1.0 MPa for the Middle Salt member and 31.1 MPa, 1.7 MPa and 0.6 MPa for the Lower Salt member.

3. Fracture Healing Experiments

Two loading schemes have been performed to assess the healing behavior of the salt fractures: uniaxial (normal) loading, and radial loading. Three types of salt fracture are simulated in the laboratory: 1) tension-induced fractures, 2) fractures formed by saw-cut surfaces, and 3) fractures formed by smooth polished surfaces. All fractures are well mated. To obtain the tension-induced fractures, the cylindrical specimens are subjected to point loading or diameter loading (Brazilian tension test). The point-loaded fracture is normal to the specimen axis, and is prepared for healing under uniaxial loading. The diameter-loaded fracture is parallel to the specimen axis, and will be healed under radial loading. The fracture formed by saw-cut surfaces is also normal to the specimen axis, while the fracture formed by polished surfaces is parallel to the specimen axis. Prior to pressurization types and amount of inclusions on the fracture surfaces have been determined and mapped. The aerial percentage of the inclusions is calculated with respect to the total fracture area. These inclusions include all associated and foreign minerals or materials that are not sodium chloride.

3.1. *Healing Under Normal Load*

Four test series with different test conditions have been performed on the saw-cut fractures. For the first two series, the normal stresses of 3.2 kPa and 3.8 kPa are applied to the saw-cut fractures under dry and saturated conditions, respectively. Three specimens are used for each normal stress. Dead weight compression machine applies constant loading on to the fracture. For the saturated condition, the fractures are submerged under saturated brine while loading. The load is removed after 30 days. No healing has been observed for both dry and saturated fractures. All saw-cut fractures remain separable.

The third and fourth test series use a normal stress of 4.3 MPa on three saw-cut fractures, and 7.8 MPa on ten tension-induced fractures. A consolidation machine with the maximum load capacity of 4 tons is used to apply constant stresses to the specimens for 30 days. The specimens are then subjected to point load testing by having the loading points lied on and parallel to the healed fracture plane. The point load strength of the healed fracture (I_H) is calculated by dividing the failure load (P) by the diameter square (D^2). The healing effectiveness (H_e) of each fracture is defined by the percentage ratio of I_H to I_S, where I_S represents the point load strength of the intact salt obtained previously from inducing the fracture to the same specimen. All specimens fail along the original fracture plane.

No healing has been detected on the saw-cut fractures tested under 4.3 MPa normal stress (test series 3). Healing however has been observed on the tension-induced fractures tested under 7.8 MPa normal stress (test series 4). Table 1 summarizes the results. Some H_e values exceed 100%. This is probably because some existing voids or fissures in salt along the fracture plane have been compressed during healing period, and subsequently strengthening the fracture beyond the previous intact condition. It should be noted that before the fractures are initially induced, the intact core specimens have not been subjected to any compression. The high variation of H_e values is probably due to the precision of the loading procedure. Even though the assessment of healing effectiveness by point load testing is relatively quick and easy, the high stress gradient induced in the specimen usually results in a high intrinsic variability of the measurement results. The complex distribution, pattern and locations of the inclusions in relation to the loading points can also enhance the variability of the strength results. The healing effectiveness tends to decrease as the amount of inclusion increases.

Table 1. Point load test results for dry salt specimens with tension-induced fractures after healing under constant normal stress of 7.8 MPa for 30 days.

Specimen No.	Inclusions (%)	Point Load Strength Index		Healing Effectiveness $H_e = [I_H/I_S] \times 100$ (%)
		Intact Salt I_S (MPa)	Salt with Healed Fracture I_H (MPa)	
e01HUT	0	0.61	1.13	185
e02HUT	30	1.05	0.75	71
e03HUT	5	0.84	1.00	119
e04HUT	40	1.09	0.40	37
e05HUT	25	0.87	0.74	85
e06HUT	10	0.56	0.59	105
e07HUT	5	1.22	0.49	40
e08HUT	5	1.25	0.48	38
e09HUT	25	0.54	0.51	94
e10HUT	15	0.56	0.40	71

3.2. *Healing Under Radial Loading*

Tension-induced fractures and polished fractures are healed under radial pressures by using overburden Poro-Perm Cell. Each fracture type is subjected to two loading configurations: static (single-step) loading and quasi-static (multi-step) loading. All specimens are tested under dry condition. During pressurization, series of gas flow permeability tests have been performed. The measured flow rate is used to calculate the hydraulic conductivity of the fracture (K_f) as a function of time, based on an assumption of the flow through parallel plates (Zeigler, 1976). The nitrogen

gas pressure is injected at a constant magnitude of 0.35 MPa. The measurement limit of the system is 10^{-8} m/s.

One polished fracture is subjected to the radial pressures (P_c) of 3.45 MPa and later increased to 6.89 MPa (quasi-static loading). Each loading takes 100 hours. This pressure scheme is repeated for the second cycle. The fracture permeability decreases with increasing radial pressures (Figure 1). Under each load, the fracture permeability also decreases with time. The second cycle of pressurization yields a lower hydraulic conductivity than do the first one, which suggessts a plastic closure of the fracture. When the pressure increases to 6.89 MPa, the hydraulic conductivity becomes lower than the limit of measurement (10^{-8} m/s).

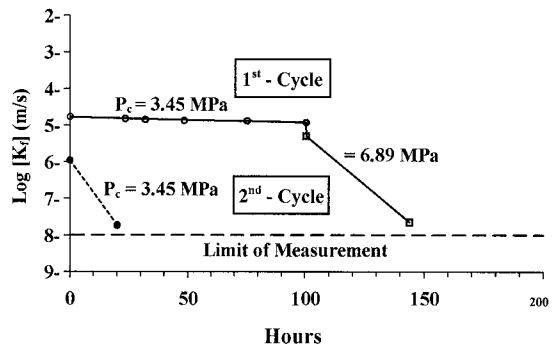

Fig. 1. Hydraulic conductivity (K_f) of polished fracture under quasi-static loading. Two loading cycles are presented.

Three tension-induced fractures have been tested under quasi-static loading. The constant radial pressures are progressively increased from 3.45, 6.89, 10.34 to 13.78 MPa. The reduction of fracture permeability with time and pressurization is found to be greater than that of the polished fracture. The permeability obtained from the second pressure cycle is notably lower than that of the first one, suggesting a significant closure of the fracture. Figures 2 and 3 show the results of quasi-static loading test for some specimens.

For the static loading test, five specimens subject to constant pressures of 0.69, 3.45, 6.98, 13.78 and 20.67 MPa. A power equation is used to fit the experimental results for each pressure level: $K_f = K_o\ (t)^{-\beta}$, where K_o represents the fracture permeability at time (t) equal to 1, and β is the time coefficient (Figure 4). The time coefficient β increases exponentially with the applied pressure (P_c): $\beta = 0.104 \cdot \exp(0.14\ P_c)$. This suggests that the reduction rate of fracture permeability is higher when the fracture subjects to a greater pressure.

It is found that healing has occurred for all tension-induced fractures after 120 hours of loading (Figure 5). The Brazilian tensile strengths of each specimen measured before and after healing are compared to assess the healing effectiveness (H_e) of the fracture. Here H_e represents the percentage ratio of the fracture tensile strength (σ_H) to the intact tensile strength (σ_B) of the same salt specimen. The tensile failure occurs along the same plane that was induced before and after healing. Table 2 summarizes the results of the healing assessment test. The polished fractures can not be effectively healed even under the pressure of 6.89 MPa for 120 hours. Healing is however found in all tension-induced fractures. Figure 6 shows the increase of H_e as the pressure (P_c) increases for the static loading test on the tension-induced fractures.

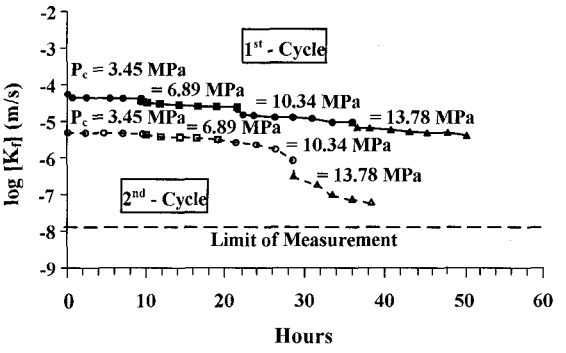

Fig. 2. Hydraulic conductivity (K_f) of tension-induced fracture as a function of time under quasi-static loading, for specimens no. HPT07e.

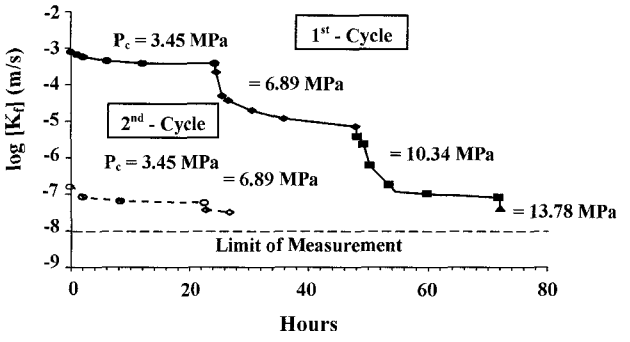

Fig. 3. Hydraulic conductivity (K_f) of tension-induced fracture as a function of time under quasi-static loading, for specimens no. HPT09e.

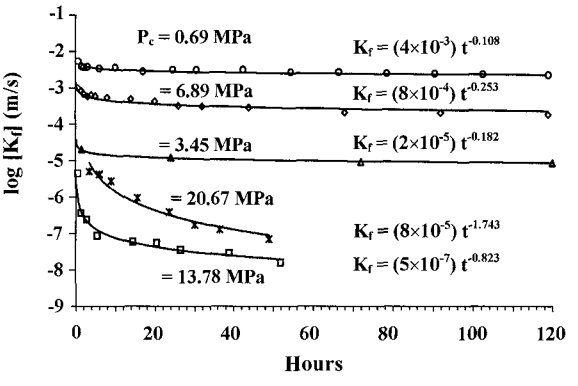

Fig. 4. Hydraulic conductivity (K_f) of five tension-induced fractures as a function of time under static loading.

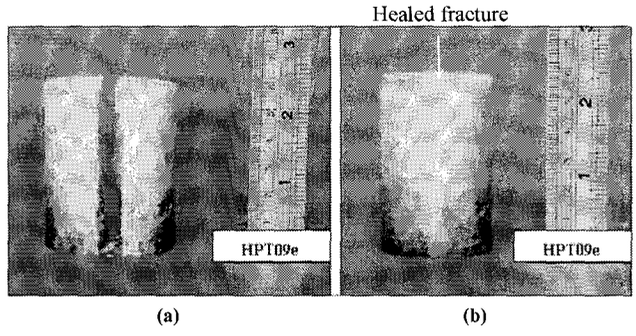

Fig. 5. Tension-induced fracture in salt prepared by diameter loading, before healing (a), and after healing (b).

Table 2. Brazilian tension test results of dry salt specimens with tension-induced fractures and polished surfaces after healing under static and quasi-static loading.

Specimen No.	Type of Fracture	Radial Pressure (MPa)	Test Duration (hrs/step)	Brazilian Tensile Strength		Healing Effectiveness $H_e = (\sigma_H/\sigma_B) \times 100$ (%)
				Intact Salt σ_B (MPa)	Salt with Healed Fracture, σ_H (MPa)	
HPT01e	Tension-Induced fracture	0.69	120	2.24	0.04	2
HPT02e		3.45	120	2.23	0.37	17
HPT03e		6.89	120	2.24	0.36	16
HPT04e		13.78	120	2.47	1.04	42
HPT05e		20.67	120	1.96	0.82	42
HPT06e	Polished surface	3.45→6.89	100	1.68	0.06	4
HPT07e	Tension-induced fracture	3.45→6.89	96	1.30	1.24	94
HPT8e		→10.34→	24	2.50	1.97	79
HPT09e		13.78	24	2.23	1.17	53

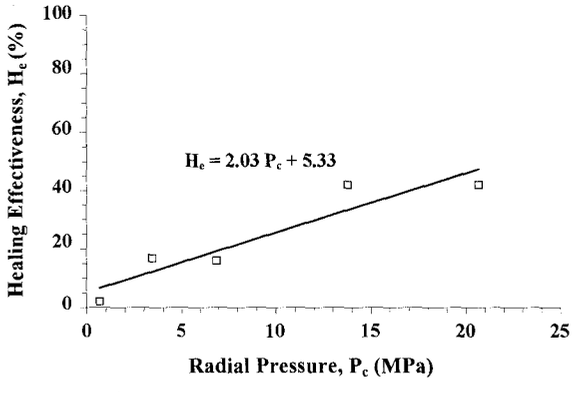

Fig. 6. Healing effectiveness (H_e) as a function of radial pressure (P_c) for tension-induced fractures after healed for 120 hours.

4. Discussions and Conclusions

The assessment of fracture healing under radial loading has an advantage over that under normal (uniaxial) loading in term of the maximum applied pressures. The applied axial load is limited by the compressive strength of the salt. The maximum axial stress used here is therefore limited to 7.8 MPa or about 30% of the strength. This is primarily to prevent the initiation of micro-cracks or fractures in the intact salt. For the radial loading test, the specimen can subject to the pressure as high as 20 MPa.

The occurrence of healing of salt fractures depends largely on the origin of the fractures. If a fracture is formed by separation or splitting of salt crystals, it can be easily healed even under relatively low stress for a short period. The splitting failure of salt crystals occurs by a separation of cleavage planes, which means that healing is likely to occur if the salt crystals on both sides of the cleavage plane return to their original position. For the fractures formed by separation of inter-crystalline boundaries, healing will not be easily achieved. In particular, if the fracture surface is coated with any inclusions, healing will not occur. This explains why the saw-cut fractures and polished fractures can not be effectively healed under the test conditions used here. It can be postulated here that healing of fracture can be enhanced by the purity of the halite crystals on the opposite sides of the fracture. This is supported by the fact that the cleavage planes inside the salt crystal are more pure than the inter-crystalline boundaries, and more than the saw-cut and polished surfaces. These artificial surfaces could be contaminated during the preparation process. To heal a saw-cut or polished salt fracture, a much higher confinement and temperature than those used here may be required.

It is not clear from the experimental results that fractures under saturated brine can be healed more effective than those under dry condition. This is because the two test conditions are applied on the saw-cut fractures and with relatively low axial stresses. For the saturated testing, it is found that re-crystallization has occurred in the fractures in form of small salt crystals. Such process however can not hold the fractures together. The specimens can be easily pulled apart by hands.

The results suggest that both pressure and time are important factors for the effectiveness of healing. The hydraulic conductivity for all salt fractures decreases with increasing applied pressure and time. This implies that fracture healing is accompanied by fracture closure. Both processes are time-dependent. The closure involves the visco-plastic deformation for the salt on both sides of the fracture. The healing involves a covalent bonding of the surfaces. It is permanent - remains even after the load has been removed. Owing to the surface smoothness, the polished fractures show a lower permeability than do the tension-induced fractures. This however does not necessarily mean that the polished fractures heal more effective than do the tension-induced fractures. A reduction of fracture permeability does not necessarily mean that the healing has occurred. This is evidenced by that even the polished fracture has been compressed until its permeability becomes lower than 10^{-8} m/s, no healing has taken place in the fracture.

Since all fractures tested here are well mated, the impact of fracture roughness can not be truly assessed. More testing is needed to confirm any mathematical relationship between the healing effectiveness and the amount and type of inclusions. For the healing assessment method, a direct tension test could be used to minimize the impact of the stress gradient induced along the fracture plane. From the results obtained here, it can be postulated that under preferable conditions (stress state, time, temperature, purity, crystal orientation, etc.), a complete healing of salt fractures is possible.

Acknowledgments

This research is funded by Suranaree University of Technology. Permission to publish this paper is gratefully acknowledged.

References

Allemandou, X. and Dusseault, M.B. (1993). "Healing Processes and Transient Creep of Salt Rock". *Geotechnical Engineering of Hard Soils-Soft Rocks.* Balkema, Rotterdam, pp. 1581-1590.

ASTM D2938-79. Standard Test Method for Unconfined Compressive Strength of Intact Rock Core Specimens. *Annual Book of ASTM Standards*, 04.08, American Society for Testing and Materials, Philadelphia.

ASTM D3967-81. Standard Test Method for Splitting Tensile Strength of Intact Rock Core Specimens. *Annual Book of ASTM Standards*, 04.08, American Society for Testing and Materials, Philadelphia.

ASTM D4543-85. Standard Practice for Preparing Rock Core Specimens and Determining Dimensional and Shape Tolerances. *Annual Book of ASTM Standards*, 04.08, American Society for Testing and Materials, Philadelphia.

ASTM D5731-95. Standard Test Method for Determination of The Point Load Strength Index of Rock. *Annual Book of ASTM Standards*, 04.08, American Society for Testing and Materials, Philadelphia.

Chan, K. S., Munson, D. E., Fossum, A. F. & Bodner, S. R. (1998). "A constitutive model for representing coupled creep, fracture and healing in rock salt", Proceeding of the 4th Conference on the Mechanical Behavior of Salt, The Pennsylvania State University, June 17-18, 1996, Clausthal-Zellerfeld, Trans Tech Publications, Germany, pp. 211-234.

Habib, P. and Berest, P. (1993). "Rock mechanics for underground nuclear waste disposal in France". *Comprehensive Rock Engineering*: Developments and case studies: Geothermal Energy and Radioactive Waste Disposal, Vol. 5, Great Britain: Pergamon, pp. 547-563.

Katz, D. L. and Lady, E. R. (1976). "Compressed Air Storage for Electric Power Generation". Richland, Washington Dept. of Energy, Pacific Northwest.

Miao, S., Wang, M. L. and Schreyer, H. L. (1995). "Constitutive Models for Healing of Materials with Application to Compaction of Crushed Rock Salt". *Journal of Engineering Mechanics*, ASCE., **10**(121): 1122-1129.

Munson, D.E., Chan, K.S. and Fossom, A.F. (1999). "Fracture and Healing of Rock Salt related to Salt Caverns". SMRI Report, Spring Meeting, Solution Mining Research Institute, Encinitas, California, April 14-16, Las Vegas, Nevada.

Ouyang, S. and Daemen, J.J.K. (1989). "Crushed Salt Consolidation". Technical Report NUREG/CR-5402, U.S. Nuclear Regulatory Commission, Washington, DC.

Renard, F. (1999). "Pressure Solution and Crack Healing and Sealing". Geology related to nuclear waste disposal, Institute of Geology and Department of Physics. Roztez, Norway: Czech Republic.

Warren, J. (1999). *Evaporites: Their Evolution and Economics.* Blackwell Science, 438 pp.

Zeigler, T.W. (1976). "Determination of Rock Mass Permeability". Technical Report S-76-2, U.S. Army Engineer Waterways Experiment Station, Vicksburg, Mississippi.